Lasers Med Sci (2014) 29:939–948
DOI 10.1007/s10103-013-1414-2

ORIGINAL ARTICLE

The effects of folate-conjugated gold nanorods in combination with plasmonic photothermal therapy on mouth epidermal carcinoma cells

Alireza Mehdizadeh · Sajjad Pandesh · Ali Shakeri-Zadeh · Seyed Kamran Kamrava · Mojtaba Habib-Agahi · Mohammad Farhadi · Morteza Pishghadam · Amirhossein Ahmadi · Sanam Arami · Yuri Fedutik

Received: 8 January 2013 / Accepted: 29 July 2013 / Published online: 7 September 2013

Abstract The use of lasers has emerged to be highly promising for cancer therapy modalities, most commonly, the photothermal therapy method. Unfortunately, the most common disadvantage of laser therapy is its nonselectivity and requirement of high power density. The use of plasmonic nanoparticles as highly enhanced photoabsorbing agents has thus introduced a much more selective and efficient cancer therapy strategy. In this study, we aimed to demonstrate the selective targeting and destruction of mouth epidermal carcinoma cells (KB cells) using the photothermal therapy of folate-conjugated gold nanorods (F-GNRs). Considering the beneficial characteristics of GNRs and overexpression of the folate receptor by KB cells, we selected F-GNRs as a targeted photothermal therapy agent. Cell viability was evaluated using a 3-(4,5-dimethylthiazol-2-yl)-2,5-diphenyltetrazolium bromide assay. Apoptosis was determined by flow cytometry using an annexin V–fluorescein isothiocyanate/propidium iodide apoptosis detection kit. No cell damage or cytotoxicity from the individual treatment of laser light or F-GNRs was observed. However, a 56 % cell lethality was achieved for KB cells using combined plasmonic photothermal therapy of 20 μM F-GNRs with seven pulses of laser light and 6-h incubation periods. Cell lethality strongly depends on the concentration of F-GNRs and the incubation period that is mainly due to the induction of apoptosis. This targeted damage is due to the F-GNRs present in the cancer cells strongly absorbing near-infrared laser light and rapidly converting it to heat. This new therapeutic avenue for cancer therapy merits further investigation using in vivo models for application in humans.

Keywords Folate-conjugated · Gold nanorod · Targeted therapy · Photothermal therapy · NIR laser light · KB cells

A. Mehdizadeh · S. Pandesh · M. Pishghadam
Department of Medical Physics, Faculty of Medicine, Shiraz University of Medical Sciences, Shiraz, Iran

A. Shakeri-Zadeh
Department of Medical Physics, School of Medicine, Iran University of Medical Sciences, Tehran, Iran

M. Habib-Agahi
Department of Medical Immunology, Shiraz University of Medical Sciences, Shiraz, Iran

A. Shakeri-Zadeh · S. K. Kamrava (✉) · M. Farhadi
Clinical Nanomedicine Laboratory, ENT–Head and Neck Research Center, Hazrat Rasoul Akram Hospital, Iran University of Medical Sciences (IUMS), Tehran, Iran
e-mail: skkamrava@yahoo.com

A. Ahmadi (✉)
Pharmaceutical Sciences Research Center, Faculty of Pharmacy, Mazandaran University of Medical Sciences, Sari, Iran
e-mail: amirhossein_pharma@yahoo.com

S. Arami
Department of Pharmaceutical Biotechnology, Faculty of Pharmacy, Tabriz University of Medical Science, Tabriz, Iran

Y. Fedutik
Department of Research & Development (R&D), PlasmaChem GmbH, Rudower Chaussee 29, 12489 Berlin, Germany

Present Address:
A. Ahmadi
Medical Nanotechnology Research Center, Faculty of Pharmacy, Tehran University of Medical Sciences, Tehran, Iran

Introduction

The use of heat has been one of the primary methods for treating tumors since its ancient usage in 1700 BC when a glowing tip of a fire drill was used for breast cancer therapy [1]. Heat sources, including focused ultrasound, laser light, and microwaves [2, 3],

can induce localized heating in a specific region, which is termed hyperthermia. Hyperthermia is defined as heating tissue to a temperature in the range of 41–47 °C [1–4]. The benefits of thermal therapeutics over conventional resection are numerous; most thermal approaches are minimally invasive or noninvasive, relatively simple to perform, and have the potential of treating embedded tumors in vital regions in which surgical resection is not feasible [2]. However, all of these heat sources have the common limitation that the heating is nonspecific. Hyperthermia can destroy both malignant and benign cells.

Among these heat sources, laser light at near-infrared (NIR) frequencies can penetrate tissues with sufficient intensity and greater spatial precision for inducing localized hyperthermia [4]. Unfortunately, laser light heating suffers from the major issue of nonspecificity. One route to improve the spatial selectivity of laser heating is to load the tumor tissue with gold nanoparticles of different shapes and structures, such as nanoshells, nanorods, nanocages, and other types of nanoparticles [5, 6]. Exposing nanoparticles to laser radiation near their plasmon-resonant absorption band makes it possible to produce localized heating of the nanoparticle-labeled cells without harming the surrounding healthy tissues [5, 7]. When the nanoparticles are irradiated, they absorb energy, which is rapidly transferred through nonradiative relaxation into heat and has accompanying effects, and this process eventually leads to irreparable damage of the cells [8, 9]. The mechanisms through which hyperthermia causes cell death include protein denaturation and the rupture of cellular membranes [10]. In addition to their enhanced absorption, scattering, and good biocompatibility, gold nanoparticles can also conjugate to a variety of biomolecular ligands, antibodies, and other targeting moieties. This property makes gold nanoparticles suitable for use in biochemical sensing and detection, medical diagnostics, and therapeutic applications [11]. To have suitable penetration in tissue for in vivo photothermal treatment, laser irradiation with a long wavelength (650–900 nm) should be used. The use of long-wavelength laser irradiation requires the maximum absorption band of the nanoparticles to be in the NIR region [12]. To improve treatment efficacy, the heat conversion efficacy of the nanoparticles should be maximized. Gold nanorods are the best option for achieving this goal. Gold nanorods are easily tuned to the NIR region by simple manipulation of their aspect ratio (length/width) and have been extensively studied for cancer therapy applications. They have the advantages of small sizes (on the order of 10×50 nm, comparable to gold colloid particles), high absorption coefficients, and narrow spectral bandwidths. Owing to their distinctive rod shape, gold nanorods have two absorption peaks corresponding to the longitudinal and transverse resonances. The transverse resonance occurs at around 520 nm, while the longitudinal resonance can span the visible and NIR wavelengths. Recent studies have investigated the photothermal heating efficiencies of NIR-absorbing gold nanoparticles, and both theoretical and experimental results have shown that nanorods offer a superior absorption cross-section versus gold–silica and gold–gold sulfide nanoparticles when normalizing for particle size differences, as well as heating per gram of gold that is at least six times faster than gold–silica nanoshells [13–15].

For better treatment, there is a need to target cancer treatments to the tumor region without damaging healthy tissue. Active targeting must be used to achieve this requirement. Active targeting is based on selectively targeting cancer cells using a specific binding site on the surface of the cell, such as a receptor [16]. A more effective and active targeting system is further needed to enhance intracellular uptake of drug containing nanocarriers within cancerous cells at the tumor site [17]. Various targeting moieties or ligands against tumor cell-specific receptors have been immobilized on the surface of nanoparticulate carriers to deliver them within cells via receptor-mediated endocytosis. Among them, vitamin folic acid (folate) has been widely employed as a targeting moiety for various anticancer drugs [18]. Folic acid drug conjugates provide a promising group of nanomaterials for active targeting [19, 20]. Folic acid (pteroylglutamate) is water-soluble. Folate is transported into both healthy and cancer cells by the folate receptors on the cell membrane. These receptors transport folate into the cytoplasm of the cell for the synthesis of thymine by dihydrofolate reductase. Cells regulate the presence of folate receptors on their surface. Cancer cells tend to overexpress the folate receptor because of their high requirements for folate. Because folate is necessary for DNA nucleotide synthesis and cell division, a cancer cell will require significantly more folate than a healthy cell. It has been proposed that the folate receptor is a suitable targeting agent because of its low expression level in healthy tissues and overexpression in cancerous tissues. An advantage offered by folate is its possible conjugation with a number of nanotechnology platforms, such as gold nanoparticles and chemotherapeutic agents [16, 19, 21, 22].

Here in this study, considering beneficial characteristics of gold nanorods, we selected such nanostructure for photothermal therapy of mouth epidermal carcinoma cells (KB cells). The laser irradiation of cells was performed at a wavelength of 755 nm. This wavelength is in the NIR region at which tissue has low absorption. Since KB cells overexpress the folate receptor, we have chosen folate-conjugated gold nanorods (F-GNRs) as a targeted nanostructure.

Materials and methods

Materials

F-GNRs were purchased from the PlasmaChem GmbH (Berlin, Germany). Trypan blue, Dulbecco's modified Eagle's medium (DMEM), Roswell Park Memorial Institute 1640 cell culture media, 3-(4,5-dimethylthiazol-2-yl)-2,5-diphenyltetrazolium bromide (MTT), dimethyl sulfoxide (DMSO), streptomycin,

penicillin, and trypsin–ethylenediaminetetraacetic acid (EDTA) were purchased from Sigma-Aldrich Corp. (St. Louis, MO, USA). Fetal calf serum (FCS) was purchased from Gibco®. The KB cell line was obtained from the Pasteur Institute of Iran, Tehran, Iran.

Preparation of GNRs functionalized with folate

GNRs with the plasmon band at 763 nm were prepared by PlasmaChem GmbH according to the study of Murphy et al., with the minor modification [23]. In order to prepare F-GNRs, 30 mg of GNRs were washed four times by water and separated on a centrifuge, after which were dispersed in 100 ml of 0.1 M cysteine aqueous solution and stirred for 12 h at room temperature. The resulting cysteine-coated GNRs were washed several times by water and dispersed into water using ultrasonic bath treatment. One hundred milligrams of folic acid was dissolved in 5 ml of DMSO. To this solution, 100 mg of *N*-hydroxysulfosuccinimide sodium salt was added. After complete dissolution, the solution was stirred for 12 h. The obtained folic acid NHS solution was added dropwise to 100 ml of the aqueous solution of GNRs. Reaction was allowed to proceed for 3 h. The obtained target product (folic acid-modified GNRs) was washed several times by water using a centrifuge and then stored as an aqueous dispersion. UV–visible (UV–vis) absorption spectroscopic measurements were recorded on a single-beam UV–vis spectrometer, Agilent 8453, using quartz cells of 1 cm path length at room temperature. The dynamic light scattering (DLS) profile was obtained by Brookhaven 90Plus Nanoparticle Size Analyzer to identify size distribution and effective diameter of nanoconjugates.

Cell culture

Our experiments were conducted on KB cells (derived from an epidermal carcinoma in the mouth of an adult Caucasian male) because of their high levels of folate receptors. The KB cell line was grown as a monolayer using the DMEM cell growth media with L-glutamine and $NaHCO_3$ supplemented with 10 % FCS, penicillin (100 U/ml), and streptomycin (100 μg/ml) in 75 cm^3 flasks. The cells were maintained in a humidified atmosphere that contained 5 % CO_2 and 95 % air at 37 °C, and the culture medium was changed every 2 days.

Light source

In this study, an alexandrite laser (Candela GentleLase) was used as the laser light source. The properties of the laser source were a wavelength of 755 nm, pulse duration of 3 ms per pulse, an energy fluence of up to 100 J/cm^2, and a spot size (diameter) range that varied between 6 and 18 mm. The treatment parameters were selected based on the results obtained during our primary pilot studies.

Cytotoxicity effects of GNRs or F-GNRs

In order to determine the KB cells confluence in culture medium, they were washed with a trypsin–EDTA solution for 5 min at 37 °C to detach any adherent cells from the surface of the flask. The cells were then resuspended in culture media, centrifuged (at 1,200 rpm for 5 min), and then manually counted with a hemocytometer and a microscope using a trypan blue staining assay to ensure their viability. The trypan blue staining method measures the number of living and dead cells in a specific volume of cells suspension (or cell density).

When the cells reached more than 85 % confluence estimated using a trypan blue staining assay, GNRs or F-GNRs at different concentrations (5, 10, and 20 μM) were dispersed in deionized water and incubated in culture medium that contained 10^6 cells/ml for different incubation periods (5, 6, and 7 h). The same density of cells without GNRs or F-GNRs was included as control group. When the incubation period was complete, the cells were centrifuged at 1,200 rpm for 5 min. The cells were then separated and plated at a density of 15,000 cells/well in flat bottom 96-well plates. MTT and annexin V binding assays were performed to evaluate the cell survival rate and induction of apoptosis, respectively.

Cytotoxicity effects of NIR laser light exposure to cells

To examine the effect of laser light on the KB cell line, cells in the absence of the nanoconjugates were exposed to different laser pulse numbers. For this reason, when the cells reached more than the desired confluence, they were plated at a density of 10^6 cells/well in flat bottom 24-well plates. The laser irradiation of each well was performed separately at a power density of 40 J/cm^2 and wavelength of 755 nm using different pulse numbers including 1, 3, 5, 7, 12, and 15 pulses for each group. The light spot covered a single well, which was considered one experimental group. These examinations were conducted to observe how different numbers of laser pulses in the absence of F-GNRs affect the cell survival rate. After exposure, the cells were incubated overnight, separated, plated at a density of 15,000 cells/well in flat bottom 96-well plates, and then evaluated cell survival rate and induction of apoptosis by performing MTT and annexin V binding assays.

Cytotoxicity effects of F-GNRs in combination with NIR laser light on KB cells

To examine the effect of combined treatment with NIR laser light and F-GNRs on the KB cell line, cells in the presence of the F-GNRs were exposed to seven pulse numbers of NIR laser. After reaching the desired confluence, the cells (10^6 cells/ml) were incubated with three different concentrations of F-GNRs for three different incubation times. After incubation, the cells were centrifuged at 1,200 rpm for 5 min. Subsequently, the treated cells were plated at a density of 10^6 cells/well in flat bottom 24-

well plates and were then exposed to seven pulses of laser light and incubated overnight. The incubated cells were then separated and plated at a density of 15,000 cells/well in flat bottom 96-well plates. MTT and annexin V binding assays were performed to evaluate the cell survival rate and induction of apoptosis.

MTT-tetrazolium assay

The viability of the KB cells was estimated using the MTT-tetrazolium assay [24–27], which measures the ability of metabolically active mitochondria in live cells to reduce a colorless tetrazolium compound to a blue formazan product. To perform this assay, the culture medium was removed. After adding 100 μl of FCS-free culture medium, 10 μl MTT was also added to each well, and the plate was incubated for 4 h. After 4 h, the culture medium was removed from the wells, and the cells were lysed in 200 μl of DMSO. Finally, the absorbance of the dissolved formazan was read at 545 nm using an ELISA reader (Stat Fax-2100 Awareness, Mountain View, CA, USA). The relative survival of the cells was represented as the absorbance of the treated sample/absorbance of the control group. The optical density of dissolved formazan is directly proportional to living cells. In our experiments, we designed control groups beside the treated groups, and therefore, the ratio of optical density (or absorbance) of the treated group to the control group is equal to cell survival. All experiments were repeated at least three times.

Detection of cell apoptotic rates by flow cytometry

The extent of apoptosis was measured through annexin V–fluorescein isothiocyanate (FITC) apoptosis detection kit as described in the manufacturer's instructions. After performing our experiments on cells, the cells were plated at a density of 200,000 cells/well in flat bottom 24-well plates. The cells were washed twice with PBS buffer and then resuspended in annexin binding buffer. Cells were then incubated with annexin V–FITC/propidium iodide (PI) in the dark for 15 min. After staining, the results were obtained using a flow cytometer and analyzed using the FlowJo software package. Viable cells were negative for both PI and annexin V–FITC; apoptotic cells were positive for annexin V–FITC and negative for PI, whereas late apoptotic dead cells displayed strong annexin V–FITC and PI labeling. Nonviable cells, which underwent necrosis, were positive for PI but negative for annexin V–FITC.

Statistical analysis

The SPSS software package (SPSS Inc., Chicago, IL, USA) for Windows® version 12.0 was used for the statistical analyses of the data. The data were analyzed for significant differences ($P<0.05$) using the Mann–Whitney test to compare all of the experimental groups. Cytotoxicity (IC_{50}) data of MTT assay were analyzed using the GraphPad computer software. The results obtained using annexin V binding assays were analyzed using the FlowJo software package. The survival curves were generated using the GraphPad Prism 5 software package.

Results

Characterization of F-GNRs

The absorption spectrum of F-GNRs (shown in Fig. 1a) presented characteristic absorption peaks of folate (280 and 360 nm). The maximum absorption peak of GNRs before conjugation with folate is 763 nm, as shown with the blue arrow in Fig. 1a. The maximum absorption peak of F-GNRs with the plasmon band in the UV–vis spectra appeared at around 780 nm, which indicated that the optical properties of GNRs were affected after functionalization with folate. Figure 1b shows the DLS profile of F-GNRs showing that the size distribution of the nanoconjugates is in the range of 30–50 nm and the effective diameter of conjugation is 40 nm.

Cytotoxicity of the GNRs or F-GNRs before NIR laser therapy

The survival percentages for KB cells incubated with different concentrations of GNRs with different incubation periods are presented in Table 1. No significant cytotoxicity ($P>0.05$) was observed, even at the highest concentrations of GNRs (20 μM) and incubation periods (7 h). The results from the cytotoxicity effects of the F-GNRs on the KB cells are presented in Table 2. Likewise, no significant cytotoxicity ($P>0.05$) was observed, even at the highest concentrations of nanoparticles (20 μM) in KB cells that overexpress the folate receptor before NIR laser therapy. The results clearly demonstrated that neither GNRs nor F-GNRs reduced the viability of KB cells in the absence of photothermal therapy.

Effects of NIR laser light exposure on cells

Figures 2 and 3 present the results of the in vitro studies on the KB cell line using an alexandrite laser without the presence of nanoparticles. The figures indicate that no significant cell lethality occurred when the number of pulses was increased up to seven pulses ($p>0.05$). Figure 2 shows that exposure of the KB cell line to the laser is harmless when up to seven pulses are applied using the listed specifications. As shown in Fig. 3, there was no significant induction of apoptosis observed in cells that were exposed to seven laser pulses (~5 %).

Photothermal studies of the GNRs and F-GNRs

Interesting results were observed when F-GNRs in combination with NIR laser light were applied in the photothermal

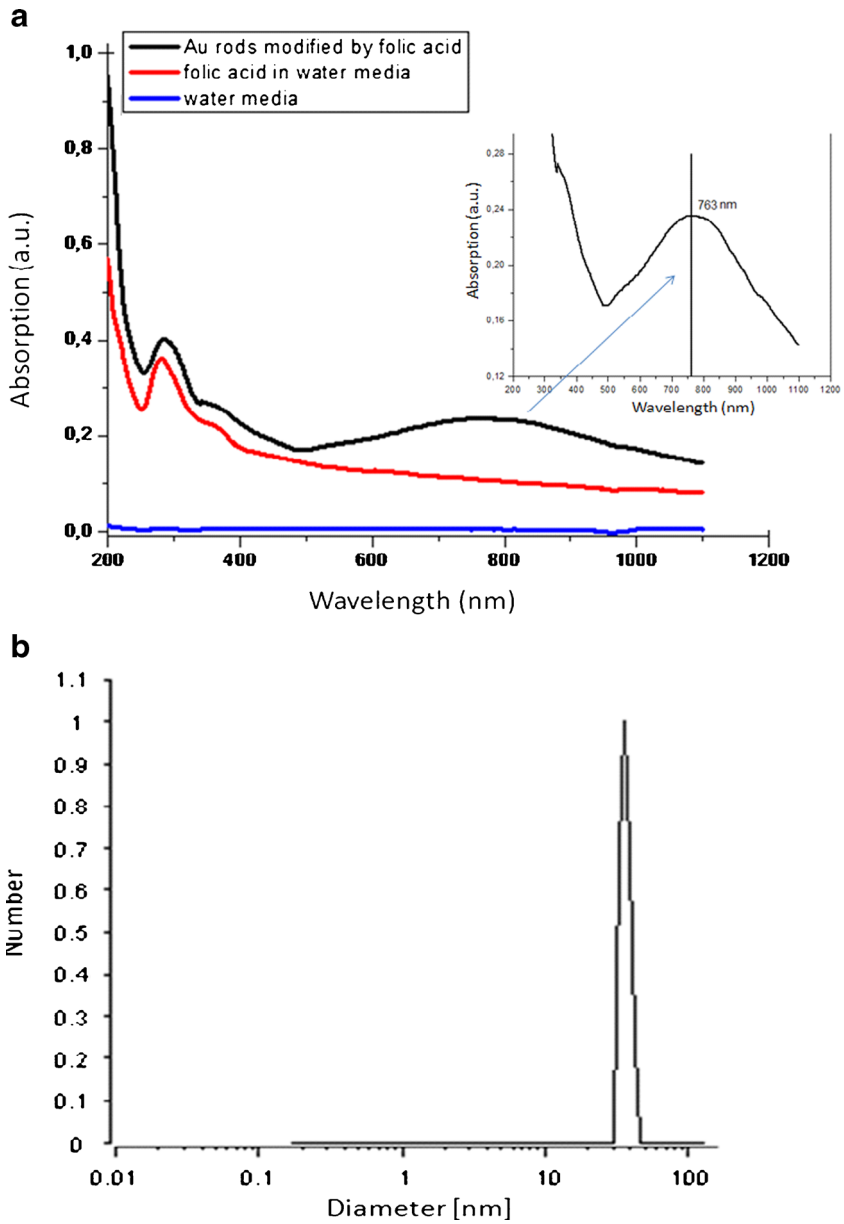

Fig. 1 **a** The absorption spectrum of F-GNRs. The maximum absorption peaks of GNRs and F-GNRs with the plasmon band in the UV–vis spectra appeared at around 763 and 780 nm, respectively. **b** DLS profile of folate-conjugated GNRs. The size distribution of F-GNRs is in the range of 30–50 nm and the effective diameter of conjugation is 40 nm

Table 1 Survival rates for KB cells incubated with different concentrations of GNRs in combination with or without seven pulses of laser

Concentration (μM)	Survival rates (5 h incubation)		Survival rates (6 h incubation)		Survival rates (7 h incubation)	
	Before laser	After laser	Before laser	After laser	Before laser	After laser
0	100±6.09	97.93±5.9	100±6.09	97.93±5.9	100±6.09	97.93±5.9
5	95.90±4.48	80.91±6.12	96.47±5.08	76.34±3.4	98.63±2.19	76.04±4.8
10	89.88±5.49	77.63±4.84	92.48±1.68	63.54±4.87	96.58±3.02	63.67±3.87
20	96.01±3.00	83.81±4.45	94.50±3.13	60.57±3.36	95.71±3.86	62.51±7.07

Data are expressed as the mean±SD. $P>0.05$, survival rates for all concentrations of GNRs in different incubation periods compared to the control sample (0 μM concentration). $P<0.05$, survival rates for all concentrations of GNRs and exposed to seven pulses of laser compared to the control sample (0 μM concentration). $P<0.05$, survival rates for all concentrations of GNRs and exposed to seven pulses of laser compared to the control sample (before expose to laser). The data were analyzed for significant differences using the Mann–Whitney test

Table 2 Survival rates for KB cells incubated with different concentrations of F-GNRs in combination with or without seven pulses of laser

Concentration (μM)	Survival rates (5 h incubation)		Survival rates (6 h incubation)		Survival rates (7 h incubation)	
	Before laser	After laser	Before laser	After laser	Before laser	After laser
0	100±6.09	97.93±5.9	100±6.09	97.93±5.9	100±6.09	97.93±5.9
5	94.95±2.76	69.67±2.53	98.14±2.51	63.91±3.84	97.70±3.26	64.95±2.87
10	95.17±4.16	56.91±5.94	96.49±2.77	57.97±1.89	96.33±2.13	58.80±1.18
20	93.58±3.24	52.69±1.39	96.40±4.29	44.30±3.13	93.24±4.68	57.22±5.97

Data are expressed as the mean±SD. $P>0.05$, survival rates for all concentrations of F-GNRs in different incubation periods compared to the control sample (0 μM concentration). $P<0.05$, survival rates for all concentrations of F-GNRs and exposed to seven pulses of laser in different incubation periods compared to the control sample (0 μM concentration). $P<0.05$, survival rates for all concentrations of F-GNRs and exposed to seven pulses of laser in different incubation periods compared to the control sample (0 μM concentration). The data were analyzed for significant differences using the Mann–Whitney test

therapy of KB cells. In Tables 1 and 2, we report the survival percentages of KB cells incubated with 0, 5, 10, and 20 μM of the GNRs or F-GNR nanoconjugates for 5, 6, and 7 h of incubation in combination with or without seven pulses of laser. The results show that the survival of cells incubated with GNRs or F-GNRs after exposure to laser light was less than that of cells before exposure to laser light (Figs. 4 and 5). Moreover, the reduced survival of cells incubated with F-GNRs is more significant than that of the cells incubated with GNRs. The percentage of live KB cells in each incubation period is dependent on the nanoconjugate dosage of F-GNRs. The greatest cell lethality was observed at a concentration of 20 μM F-GNRs and an incubation period of 6 h after exposure to laser light (Fig. 5). The induction of apoptosis significantly increased after exposure to laser light in cells incubated with GNRs or F-GNRs (Figs. 6 and 7). In addition, the apoptosis induction of cells incubated with F-GNRs in the presence of NIR laser light is more significant than that of the cells incubated with GNRs.

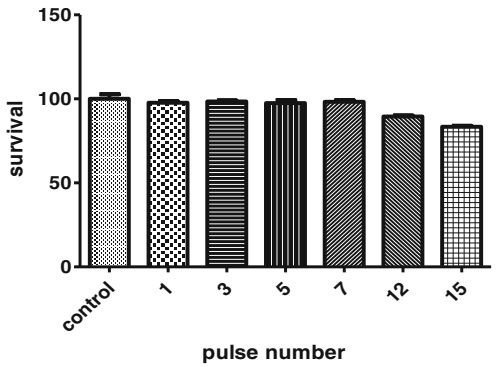

Fig. 2 The survival percentages of KB cells following exposure to different numbers of laser pulses with the following properties: 15 mm diameter spot size, 40 J/cm^2 fluence, 755 nm wavelength, and 3 ms pulse durations. The laser was not exposed to the control group, and we considered this group for evaluating other parameter on cell lethality. ***$P<0.001$, survival rates for KB cells exposed to 15 pulses of laser compared to the control sample (0 pulse). The data were analyzed for significant differences using the Mann–Whitney test

Discussion

Photothermal therapy is in part based on photodynamic therapy, in which photosensitive dyes can be selectively retained and accumulated in specific tissues or cells. With sufficient light irradiation, the dye can be brought to an excited state where it releases vibrational energy (heat). Unlike the conventional methods for cancer treatment (e.g., surgical removal, radiotherapy, chemotherapy), photothermal treatment only leads to the selective destruction of cancer cells via hyperthermia, but with minimal injury to the surrounding healthy cells. As reported in the literature, GNRs has recently been one of the promising materials for use in various biomedical applications, especially for imaging and cancer hyperthermia because of their biocompatibility and tunable light absorption properties [28]. Shukla et al. suggested that colloidal gold nanospheres do not show any cytotoxic effect up to 100 μM concentration, even after incubation for up to 72 h with RAW264.7 macrophage cells [29]. There are, at present, only a few other publications considering the possible cytotoxicity of gold nanoparticles and even fewer that specifically address

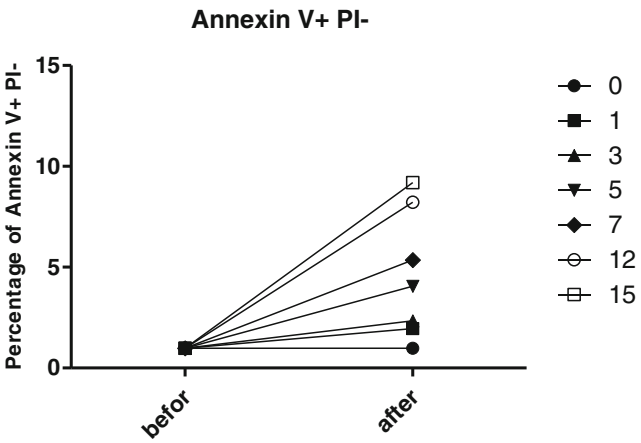

Fig. 3 The binding percentage of annexin V to cells irradiated with different numbers of laser pulses. The flow cytometry results of cell exposure to different numbers of pulses

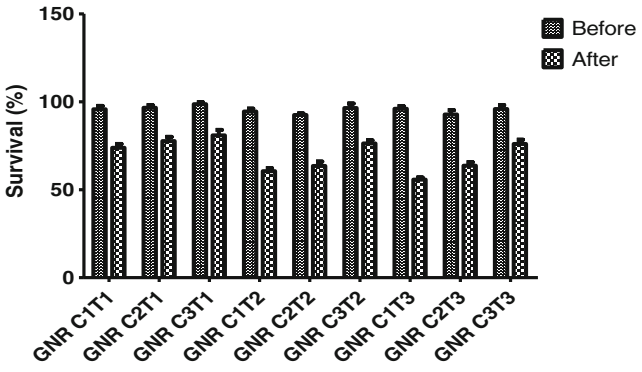

Fig. 4 The survival percentages obtained for the KB cells before and after photothermal treatment with various GNR concentrations and incubation periods (C1=20 μM, C2=10 μM, and C3=5 μM; T1=5 h, T2=6 h, and T3=7 h)

gold nanorods. But, there is evidently still some statistically important reduction of cell viability due to the nanorods, particularly if at higher concentration [30]. Nevertheless, in our study, no significant cytotoxicity was induced in KB cells by the GNRs up to 20 μM concentration. This result indicates that GNRs is safe for cells in the absence of light irradiation, even over incubation times up to 7 h.

However, the GNRs in the presence of appropriate light irradiation produce high temperatures. The level of temperature produced by GNRs impregnated inside cancerous cells can be controlled by the level and duration of radiation in order to photothermally kill the cells [16]. In photothermal cancer therapy, the fast and intensive internalization by cancer cells is one of most important factors. Efficient transformation of NIR by GNRs to heat energy and their easy bioconjugation determine their use as good photothermal agents in cancer cell targeting. In spite, there is also a potential problem in so far as nonspecific uptake of gold nanorods might cause interference. Therefore, it appears important to avoid nonspecific uptake and accumulation of gold nanorods. Specificity of effect and selective targeting

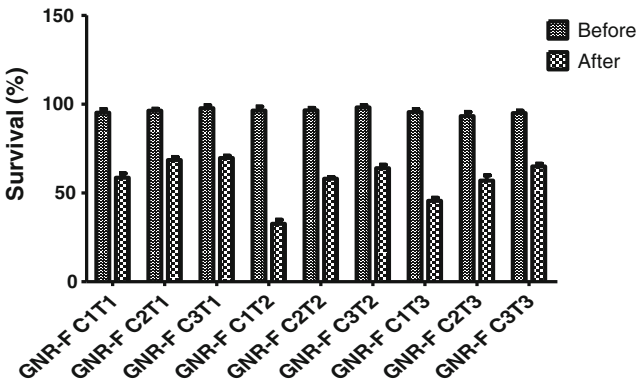

Fig. 5 The survival percentages obtained for the KB cells before and after photothermal treatment for different F-GNR concentrations and various incubation periods (C1=20 μM, C2=10 μM, and C3=5 μM; T1=5 h, T2=6 h, and T3=7 h)

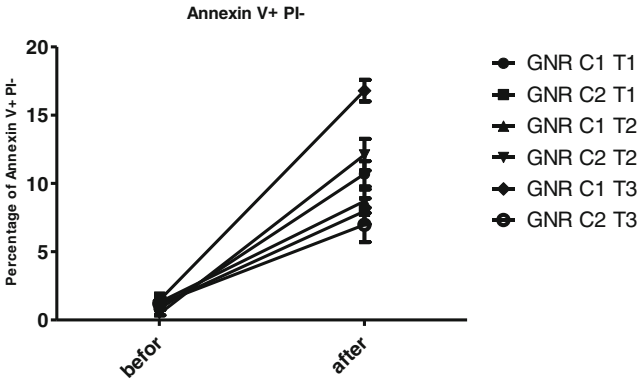

Fig. 6 The binding percentage of annexin V to cells incubated with GNRs of different concentrations and incubation periods before and after photothermal treatment (C1=20 μM and C2=10 μM; T1=5 h, T2=6 h, and T3=7 h). $P<0.05$, percentage of annexin $V^{+}PI^{-}$ as the index of apoptotic cells for all concentrations of GNRs and exposed to seven pulses of laser compared to the control sample (before expose to laser)

can be achieved, generally by functionalization of the gold nanorods with a biomolecule [28].

In 2007, Huff et al. [31] used GNRs coated with cetyltrimethylammonium bromide (CTAB) for rapid and irreversible internalization by KB cells. Although this coating material increases the cellular uptake level, it exhibits considerable toxicity. In another study, Huff et al. demonstrated that plasmon-resonant GNRs, which have large absorption cross-sections in NIR frequencies, were excellent candidates as multifunctional agents for image-guided therapies based on localized hyperthermia. The authors observed that the controlled modification of the surface chemistry of the NRs is of critical importance as issues of cell-specific targeting and nonspecific uptake must be addressed before clinical evaluation. Nanorods coated with CTAB were internalized within hours into KB cells by a nonspecific uptake pathway. In contrast, the careful removal of CTAB from the NRs functionalized with folate resulted in their

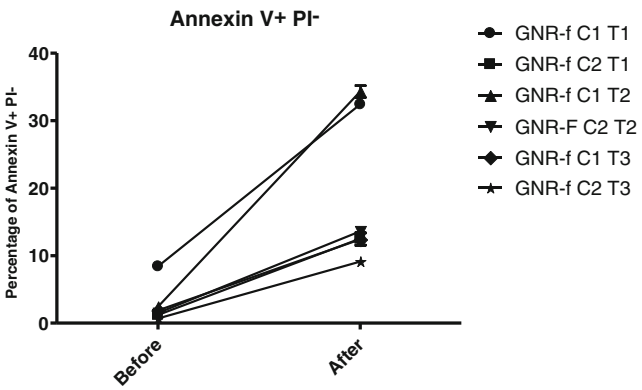

Fig. 7 The binding percentage of annexin V to cells incubated with F-GNRs of different concentrations and incubation periods before and after photothermal treatment (C1=20 μM and C2=10 μM; T1=5 h, T2=6 h, and T3=7 h). $P<0.05$, percentage of annexin $V^{+}PI^{-}$ as the index of apoptotic cells for all concentrations of F-GNRs and exposed to seven pulses of laser compared to the control sample (before expose to laser)

accumulation on the cell surface over the same time interval [4]. Therefore, Folic acid can be used for active tumor targeting because cancer cells require excessive folic acid, which is a ligand for folate receptors [4, 32].

Mansoori et al. [16] used two types of F-GNPs for the selective targeting of folate receptor-positive cancerous cells. Upon receiving intense pulsed light, a greater killing of cells was observed in human adenocarcinoma (HeLa) cells than in MCF-7 cells. HeLa cells are known to overexpress folate receptors [33], while MCF-7 is known as a very-low-level folate receptor expression cell [34]. Actually, in the research of Mansoori et al., preferential targeting to cancerous cells by the two nanoconjugates was studied by comparing the results obtained from HeLa and MCF-7 cell lines. This result demonstrated that folate targeting is effective for selective cancer cells targeting in which folate receptors are overexpressed. Huff et al. have also conjugated folate ligands with oligo(ethylene glycol) spacers to gold nanorods by in situ dithiocarbamate formation. The F-GNRs were found to specifically bind to the surface of KB cancer cells [4]. In this regard, doxorubicin nanoaggregates delivered using folate receptor targeting [21]. The authors produced doxorubicin–polyethylene glycol–folate conjugates and exposed them to folate moieties that were overexpressed on the surface of KB cancer cells. In this study, it was demonstrated that the doxorubicin nanoaggregates exhibited a greater extent of intracellular uptake against folate receptor-positive cancer cells than folate receptor-negative cells, which indicates that the cellular uptake occurs via a folate receptor-mediated endocytosis mechanism. A previous study also used GNRs for heat-induced tumor cell death studies. In their study, the authors designed nanorods that contain folate moieties on their surface targeted toward the plasma membrane of malignant KB cells and NIH-3 T3 cells, which express high and low folate receptor levels on their surfaces, respectively. As expected, in contrast to the INH-3 T3 cells, the KB cells were densely coated with the F-GNRs. Photothermolysis was investigated after laser irradiation of the cells, and the results indicated that degradation of the actin network causes considerable degradation of the plasma membrane integrity, which leads to specified cell death [35].

In our study, to improve the cell-specific targeting of GNRs by cancer cells, the GNRs were conjugated with folate to target KB cells overexpress the folate receptor. Hence, the KB cells were incubated with F-GNRs and then exposed to continuous seven pulses of NIR laser (wavelength of 755 nm) at 40 J/cm^2 fluence. No photothermal destruction is observed on the cells in the absence of nanoconjugate at the same energy required to kill the cells with F-GNRs conjugate bonded. F-GNRs thus offer a novel type of selective photothermal agents using a NIR laser at low powers. And the MTT data showed that, upon different times of incubation, the F-GNRs in a concentration-dependent manner could suppress the proliferation and growth of KB irradiated with NIR laser and more than 50 % cells can be killed when the incubation time was 6 h at 20 μM of F-GNRs.

Tong et al. have proven this to be useful for characterizing the cellular uptake of GNRs. This study involves the targeted delivery of F-NRs to KB cells overexpressing the high-affinity folate receptor, which is known to internalize folic acid conjugates by receptor-mediated endocytosis. Upon incubation with KB cells for 6 h prior to TPL imaging, F-NRs were present in high density on the surface of the outer membrane [35]. This is totally consistent with the results of our photothermal treatment of KB cells with F-NGPs, in which maximum cell death was observed after 6 h of incubation.

In another study, the GNRs were conjugated with the folate (F-GNRs) and targeted to the hepatocarcinoma cell line ($HepG_2$). In this report, the photothermal effects of the particles on the $HepG_2$ cell line were investigated using MTT assay, flow cytometry, cell morphology assays, cytoskeleton, cell surface adhesion, and stiffness at the subcellular level. The authors observed that NIR laser-induced hyperthermia of F-GNRs could break the cell membrane integrity and homeostasis and subsequently lead to depolymerization of the cytoskeleton and an influx of intracellular calcium ions. The immunofluorescence images also confirmed that cytotoxicity was associated with the involvement of apoptosis and reorganization of the cytoskeleton [28]. The conjugation and adsorption on the cell membrane is presumably mediated by multivalent binding to the folate receptors on the cell surface, a widely used system for targeted delivery to tumor cells [32, 36]. On the other hand, the F-GNRs mostly located in/on the cell membrane or cytoplasm but not nuclear. As Lovrić reported, green QDs (entered the nucleus) were significantly more toxic than red QDs (distribution in cytoplasm) tested in PC12 cells. Therefore, this also implied that F-GNRs had little inherent cytotoxicity [37], which was consistent with the MTT result in our study.

In previous experiments using laser energy and gold nanoparticles to kill cancer cells, a maximal thermal effect with 30- to 40-nm size particles was observed [38]. In accordance, our study showed that the size distribution of F-GNRs was in the range of 30–50 nm and the effective diameter of conjugation is 40 nm (Fig. 1b).

To ascertain whether or not the inhibitory effect was associated with the induction of apoptosis, staining cells with annexin V–FITC and PI labeling were performed. Percentage of annexin V^+PI^- as the index of apoptotic cells for all concentrations of F-GNRs and exposed to seven pulses of laser was significantly increased compared to the control sample (before expose to laser). Plasma membrane phospholipids are asymmetrically distributed between inner and outer leaflets of the plasma membrane. Thus, while phosphatidylcholine and

sphingomyelin are exposed on the external surface of the lipid bilayer, phosphatidylserine is located on the inner surface. It has been shown recently that loss of phospholipids asymmetry, leading to exposure of phosphatidylserine on the outside of the plasma membrane, is an early event of apoptosis. The anticoagulant annexin V preferentially binds to negatively charged phospholipids such as phosphatidylserine. By conjugating fluorescein to annexin V, it has been possible to use such a marker to identify apoptotic cells by flow cytometry. During apoptosis, the cells become reactive with annexin V after the onset of chromatin condensation but prior to the loss of the plasma membrane ability to exclude PI. Therefore, by staining cells with a combination of fluoresceinated annexin V and PI, it is possible to detect nonapoptotic live cells (annexin V-negative, PI-negative), early apoptotic cells (annexin V-positive, PI-negative), and late apoptotic or necrotic cells (PI-positive) by flow cytometry [39]. In our study, the induction of apoptosis significantly increased after exposure to laser light in cells incubated with F-GNRs, as shown in the annexin V binding assay results. Therefore, the reduction in cell survival that was observed during the MTT assay is primarily due to apoptosis.

Because the F-GNR nanoconjugate material contains folate, it can be applied to selectively target folate receptor-positive cancer cells, which overexpress the folate receptor on their surface. The significant absorption of this nanoconjugate makes it a promising material for use in cancer therapy and the thermal ablation of tumors. We have experimentally demonstrated a method for selective nanophotothermolysis using folate-conjugated GNRs. The method was applied to the KB cell line. An alexandrite laser was used to heat the F-GNRs nanoconjugate, and promising results were obtained.

Conclusion

No significant cytotoxicity was induced in KB cells by different concentrations of GNRs and F-GNR nanoconjugates. This result indicates that these nanoparticles are safe for cells, even over incubation times up to 7 h. Exposure of the KB cell line to an alexandrite laser (up to seven pulses) was observed to be safe for cells that were not incubated with GNRs or F-GNRs utilizing the procedure introduced here. However, a 56 % cell lethality was achieved for KB cells using combined plasmonic photothermal therapy of 20 μM F-GNRs with seven pulses of laser light and 6-h incubation periods. From our results, it is obvious that reduction in cell survival is mainly due to the induction of apoptosis, and this is an advantage for our photothermal treatment. This targeted damage is due to the F-GNRs present in the cancer cells strongly absorbing NIR laser light and rapidly converting it to heat. This new therapeutic avenue for cancer therapy merits further investigation using in vivo models for application in humans.

References

1. Huang X, Jain PK, El-Sayed IH, El-Sayed MA (2008) Plasmonic photothermal therapy (PPTT) using gold nanoparticles. Lasers Med Sci 23:217–228
2. O'Neala DP, Hirschb LR, Halasc NJ, Paynea JD, Westb JL (2004) Photo-thermal tumor ablation in mice using near infrared-absorbing nanoparticles. Cancer Lett 209:171–176
3. El-Sayeda IH, Huangb X, El-Sayed M (2006) Selective laser photothermal therapy of epithelial carcinoma using anti-EGFR antibody conjugated gold nanoparticles. Cancer Lett 239:129–135
4. Huff TB, Tong L, Zhao Y, Hansen MN, Cheng JX, Wei A (2007) Hyperthermic effects of gold nanorods on tumor cells. Nanomedicine (Lond) 2:125–132
5. Terentyuk GS, Maslyakova GN, Suleymanova LV, Khlebtsov NG, Khlebtsov BN, Akhchurin GG et al (2009) Laser-induced tissue hyperthermia mediated by gold nanoparticles: toward cancer phototherapy. J Biomedical Optics 14:021016
6. Pitsillides CM, Joe EK, Wei X, Anderson RR, Lin CP (2003) Selective cell targeting with light-absorbing microparticles and nanoparticles. Biophys J 84:4023–4032
7. Letfullin RR, Joenathan C, George TF, Zharov VP (2006) Laser-induced explosion of gold nanoparticles: potential role for nanophotothermolysis of cancer. Nanomedicine (Lond) 1:473–480
8. Zharov VP, Melcer KE, Galitovskaya EN, Smeltzer MS (2006) Photothermal nanotherapeutics and nanodiagnostics for selective killing of bacteria targeted with gold nanoparticles. Biophys J 90:619–627
9. Tong L, Wei Q, Wei A, Chen JX (2009) Gold nanorods as contrast agents for biological imaging: optical properties, surface conjugation and photothermal effects. Photochem Photobiol 85:21–32
10. Day ES, Thompson PA, Zhang L, Lewinski NA, Ahmed N, Drezek RA et al (2011) Nanoshell-mediated photothermal therapy improves survival in a murine glioma model. J Neurooncol 104:55–63
11. Jain PK, Lee KS, El-sayed IH, El-sayed MA (2006) Calculated absorption and scattering properties of gold nanoparticles of different size, shape, and composition: applications in biological imaging and biomedicine. J Phys Chem 110:7238–7348
12. Huang X, El-Sayed IH, El-Sayed MA (2006) Cancer cell imaging and photothermal therapy in the near-infrared region by using gold nanorods. J Am Chem Soc 128:2115–2120
13. Cole JR, Mirin NA, Knight MW, Goodrich GP, Halas NJ (2009) Photothermal efficiencies of nanoshells and nanorods for clinical therapeutic applications. J Phys Chem C 113:12090–12094
14. Jain PK, Lee KS, El-Sayed IH, El-Sayed MA (2006) Calculated absorption and scattering properties of gold nanoparticles of different size, shape, and composition: applications in biological imaging and biomedicine. J Phys Chem B 110:7238–7248
15. Von Maltzahn G, Park JH, Agrawal A, Bandaru NK, Das SK, Sailor MK et al (2009) Computationally guided photothermal tumor therapy using long-circulating gold nanorod antennas. Cancer Res 69:3892–3900
16. Mansoori GA, Brandenburg KS, Shakeri-Zadeh A (2010) A comparative study of two folate-conjugated gold nanoparticles for cancer nanotechnology applications. Cancers 2:1911–1928
17. Weitman SD, Weinberg AG, Coney LR, Zurawski VR, Jennings DS, Kamen BA (1992) Cellular localization of the folate receptor: potential role in drug toxicity and folate homeostasis. Cancer Res 52:6708–6711
18. Reddy JA, Low PS (2000) Enhanced folate receptor mediated gene therapy using a novel pH-sensitive lipid formulation. J Control Release 64:27–37
19. Shakeri-Zadeh A, Ghasemifard M, Mansoori GA (2010) Structural and optical characterization of folate conjugated gold nanoparticle. Physica E 42:1272–1280

20. Mc Neil SE (2005) Nanotechnology for the biologist. J Leukoc Biol 78:585–594
21. Yoo HS, Park TG (2004) Folate-receptor-targeted delivery of doxorubicin nano-aggregates stabilized by doxorubicin–PEG–folate conjugate. J Controlled Release 100:247–256
22. Ghaghada KB, Saul J, Natarajan JV, Ballamkonda RV, Annapragada AV (2006) Folate targeting of drug carriers: a mathematical model. J Controlled Release 104:113–128
23. Murphy CJ, Sau TK, Gole AM, Orendorff CJ, Gao J, Gou L, Hunyadi SE, Li T (2005) Anisotropic metal nanoparticles: synthesis, assembly, and optical applications. J Phys Chem B 109:13857–13870
24. Sazgarnia A, Montazerabadi AR, Bahreyni-Toosi MH, Ahmadi A (2013) Photosensitizing and radiosensitizing effects of mitoxantrone: combined chemo-, photo-, and radiotherapy of DFW human melanoma cells. Lasers Med Sci. doi:10.1007/s10103-013-1275-8
25. Montazerabadi AR, Sazgarnia A, Bahreyni-Toosi MH, Ahmadi A, Shakeri-Zadeh A, Aledavood A (2012) Mitoxantrone as a prospective photosensitizer for photodynamic therapy of breast cancer. Photodiagnosis Photodyn Ther 9:46–51
26. Montazerabadi AR, Sazgarnia A, Bahreyni-Toosi MH, Ahmadi A, Aledavood A (2012) The effects of combined treatment with ionizing radiation and indocyanine green-mediated photodynamic therapy on breast cancer cells. J Photochem Photobiol, B 109:42–49
27. Sazgarnia A, Montazerabadi AR, Bahreyni-Toosi MH, Ahmadi A, Aledavood A (2013) In vitro survival of MCF-7 breast cancer cells following combined treatment with ionizing radiation and mitoxantrone-mediated photodynamic therapy. Photodiagnosis Photodyn Ther 10:72–78
28. Jin H, Yang P, Cai J, Wang J, Liu M (2012) Photothermal effects of folate-conjugated Au nanorods on HepG2 cells. Appl Microbiol Biotechnol 94:1199–1208
29. Shukla R, Bansal V, Chaudhary M, Basu A, Bhonde RR, Sastry M (2005) Biocompatibility of gold nanoparticles and their endocytotic fate inside the cellular compartment: a microscopic overview. Langmuir 21:10644–10654
30. Takahashi H, Niidome Y, Yamada S (2005) Controlled release of plasmid DNA from gold nanorods induced by pulsed near-infrared light. Chem Commun (Camb) 7:2247–2249
31. Huff TB, Hansen MN, Zhao Y, Cheng J, Wei A (2007) Controlling the cellular uptake of gold nanorods. Langmuir 23:1596–1599
32. Leamon CP, Reddy JA (2004) Folate-targeted chemotherapy. Adv Drug Deliv Rev 56:1127–1141
33. Masters JR (2002) HeLa cells 50 years on: the good, the bad and the ugly. Nat Rev Cancer 2:315–319
34. Chung K, Saikawa Y, Paik T, Dixon KH, Mulligan T, Cowan KH et al (1993) Stable transfectants of human MCF-7 breast cancer cells with increased levels of the human folate receptor exhibit an increases sensitivity to antifolates. J Clin Invest 91:1289–1294
35. Tong L, Zhao Y, Huff TB, Hansen MN, Wei A, Cheng JX (2007) Gold nanorods mediate tumor cell death by compromising membrane integrity. Adv Mater 19:3136–3141
36. Kamen BA, Smith AK (2004) A review of folate receptor alpha cycling and 5-methyltetrahydrofolate accumulation with an emphasis on cell models in vitro. Adv Drug Deliv Rev 56:1085–1097
37. Lovrić J, Bazzi HS, Cuie Y, Fortin GRA, Winnik FM, Maysinger D (2005) Differences in subcellular distribution and toxicity of green and red emitting CdTe quantum dots. J Mol Med 83:377–385
38. Zharov VP, Galitovsky V, Viegas M (2003) Photothermal detection of local thermal effects during selective nanophotothermolysis. Appl Phys Lett 83:4897–4899
39. Endersen PC, Prytz PS, Aarbakke J (1995) A new flow cytometric method for discrimination of apoptotic cells and detection of their cell cycle specificity through staining of F-actin and DNA. Cytometry 20:162–171